

# Evaluation of IFS Model for Tropical Cyclone Forecasting in Vietnam: Track, Intensity, and Rainfall (2018–2022)

Le, T. T. H.,<sup>1</sup> Hoang, T. V.,<sup>2\*</sup> Nguyen, T. H.,<sup>1</sup> Tran, T. D.<sup>1</sup> and Nguyen, T. D. H.<sup>3</sup>

<sup>1</sup>Viet Nam Meteorological and Hydrological Administration, Vietnam

E-mail: leha246@gmail.com, nthang0676@gmail.com,\* trantiendatk54@gmail.com

<sup>2</sup>College of Construction and Development, Feng Chia University, Taiwan

E-mail: tvhoang@o365.fcu.edu.tw

<sup>3</sup>Hanoi University of Natural Resources and Environment, Vietnam, E-mail: ntdhien@hunre.edu.vn

\*Corresponding Author

DOI: <https://doi.org/10.52939/ijg.v21i12.4643>

## Abstract

*This study evaluates the forecasting performance of the Integrated Forecasting System (IFS) model developed by the European Centre for Medium-Range Weather Forecasts (ECMWF) in predicting tropical cyclones (TCs) affecting Vietnam during the period 2018–2022. The assessment focuses on TC track, intensity, and rainfall forecasts, employing best-track data from the Regional Specialized Meteorological Center (RSMC) Tokyo and rainfall observations collected from 186 meteorological stations across Vietnam. The results show that the mean direct position error (DPE) increases with forecast lead time, from 71 km at 24 hours to 118 km at 48 hours and 183 km at 72 hours. A statistically significant downward trend is observed at the 48-hour forecast horizon, indicating improvement in track accuracy. Overall, these errors remain within the acceptable operational thresholds for Vietnam, confirming the model's applicability for routine forecasting. In terms of TC intensity, forecast errors show limited variation across different lead times, with the mean absolute error (MAE) of  $V_{max}$  averaging 9 knots (4.63 m/s) and the root mean square error (RMSE) of  $V_{max}$  averaging 12 knots (6.17 m/s). Both values are consistent with national standards; however, a few cases exhibited substantial deviations, particularly for rapidly intensifying cyclones. For TC-induced rainfall, the IFS model demonstrates the highest skill in forecasting light rainfall (<16 mm) across all lead times, whereas predictive skill declines notably for heavier rainfall categories. At a 72-hour lead time, both the threat score (TS) and the probability of detection (POD) drop below 0.10 for rainfall exceeding 50 mm, underscoring considerable limitations in forecasting heavy and very heavy precipitation events.*

**Keywords:** ECMWF-IFS, Rainfall, Tropical Cyclone Intensity

## 1. Introduction

Tropical cyclones (TCs) are among the most hazardous weather phenomena affecting Vietnam's mainland. On average, Vietnam experiences six to seven TCs each year [1]. Between 1977 and 2017, typhoons with wind speeds exceeding 20 knots struck Vietnam 105 times [2]. In 2024, Typhoon Yagi and the subsequent flooding resulted in 320 fatalities, 25 missing persons, and 1,978 injuries. Additionally, 283,383 houses were damaged, 122,415 homes were flooded, and 3,755 schools along with 852 healthcare facilities were affected [3]. Due to their intensity, widespread impact, and unpredictability, TCs and other natural hazards have caused substantial losses of life and property across

the country. The National Center for Hydro-Meteorological Forecasting (NCHMF) has significantly enhanced its TC forecasting capability, particularly for track and intensity prediction, through the implementation of advanced numerical weather prediction systems. These include the Cray XC40 supercomputer for high-resolution simulations, data assimilation from satellite, radar, and surface observations, and the SmartMet visualization platform. In addition, artificial intelligence techniques are being applied to improve short-term forecasts of TC behavior over the East Sea and Vietnam.

Several numerical models are currently employed for TC forecasting in Vietnam, among which the Integrated Forecasting System (IFS) developed by the European Centre for Medium-Range Weather Forecasts (ECMWF) has demonstrated notable skill in representing complex TC scenarios, such as recurring tracks and interactions with complex terrain [4]. IFS products play a crucial role in operational forecasting and early warning activities, with comparative studies showing that the IFS provides more accurate track forecasts than other models such as the Global Forecast System (GFS) and the Global Spectral Model (GSM) [4].

Operationally, the IFS model is utilized in Vietnam for daily weather forecasting, extreme rainfall prediction [5], temperature forecasting [6], and drought warning [7]. Since 2014, the implementation of a 9 km resolution (an improvement over the previous 14 km configuration) has significantly enhanced TC track forecasts [8]. The IFS model's effectiveness lies in its high spatial resolution and its ability to capture large-scale atmospheric circulation patterns both essential for forecasting within Vietnam's complex topography and diverse climatic regions.

Moreover, IFS forecast products have been integrated with hydrological and coupled models, such as MIKE SHE for reservoir inflow prediction and WRF3KM-IFS-DA or MIKE URBAN for urban flood simulation, demonstrating improved forecast performance across multiple lead times and case studies [9] and [10]. Although research in Vietnam has confirmed the IFS model's potential to improve forecast quality, its performance tends to deteriorate as the forecast lead time increases. According to Tran Duc Ba [5], forecast accuracy declines with higher rainfall intensities, and the IFS exhibits reduced reliability at 72-hour lead times. These findings indicate that evaluations of IFS performance, particularly regarding TC-related rainfall in Vietnam, remain limited and merit further investigation.

Previous international studies [11] and [12] have also examined the forecasting capability of the IFS model, reporting its effectiveness for both meteorological and hydrological applications. While the model performs well in short-term forecasts, its accuracy decreases with extended lead times. Specifically, it tends to overestimate light and moderate rainfall while underestimating heavy and extreme precipitation events. Additionally, the IFS predicts minimum and average temperatures more accurately than maximum temperatures across most regions of Vietnam. Such biases in precipitation and temperature forecasts may affect the model's capacity to realistically simulate TC intensity and

associated rainfall distribution both critical components in TC forecasting.

TC track forecasts provide critical information about the cyclone's strength, potential impacts (e.g., heavy rainfall-induced flooding, landslides, storm surge, wind damage, and coastal erosion), and the spatial extent of its effects on both land and marine environments. While track forecasts have improved significantly, forecasting cyclone intensity remains a persistent challenge, largely due to the involvement of processes such as internal structural evolution and rapid changes in strength, which are difficult to observe and simulate accurately. Accurate prediction of TC track and intensity is essential for mitigating impacts and reducing loss of life and property. However, forecast errors in both track and intensity remain, primarily due to uncertainties in the initial atmospheric state and limitations in representing complex TC structure and evolution. Several studies have suggested these errors result from uncertainties in the atmospheric state during the forecasting process as well as imperfections in the models [13] and [14]. Specifically, previous research examined tropical cyclone track forecasts in the northwest Pacific basin and identified four primary sources of error, including asymmetries in cyclone circulation, variations in storm intensity, and expansions of the subtropical high [15]. Other studies have shown that improvements in tropical cyclone intensity forecasting remain challenging due to errors in simulating inner-core structures, uncertainties in initial conditions arising from insufficient air-sea coupling, and limited understanding of rapid intensity changes [16]. Rather than conducting an in-depth analysis of the underlying causes of forecast errors in tropical cyclone track and intensity, this study focuses on evaluating the performance of the IFS model in predicting these two key aspects, thereby contributing to a better understanding of its operational applicability in Vietnam.

The substantial variability and asymmetry of tropical cyclone rainfall during landfall shaped by vertical wind shear, storm motion speed, surface processes, extra-tropical transition, and humidity [17]. There have been significant improvements in forecasting the track, intensity, and landfall of TCs, but challenges remain in estimating and predicting TC rainfall. As a result of the unique dynamics of TC clouds, these challenges are due to the high spatiotemporal variability and asymmetric distribution of TC rainfall. As well, TC rainfall is affected by factors such as topography, the translation speed and direction of the TC, as well as its interactions with troughs and ridges, resulting in errors in peak intensity and distribution. Eight key factors have been identified as influencing TC

rainfall forecasting: cyclone motion, cyclone size, topography, humidity, atmospheric instability, diurnal cycles (with peak rainfall near the cyclone center typically occurring at night and outer rainbands during the day), vertical wind shear, and various interactions involving troughs, fronts, jets, and extratropical transitions [18]. Meteorologists continue to face significant challenges despite significant advancements in recent years. Advances in tropical cyclone (TC) rainfall forecasting have been summarized, including improved understanding of the contribution of TC rainfall to global precipitation [19]; detailed analyses of TC rainband dynamics [20][21][22][23] and [24]; investigations into environmental influences on TC rainfall processes, including vertical wind shear (VWS) [25] and [26] and the role of topography [27]; studies examining the relationship between TC rainfall, storm intensity, and storm structure [28][29] [30][31][32] and [33]; improvements in numerical weather prediction (NWP) rainfall simulation through increased model resolution [34][35][36] and [37]; efforts to reduce uncertainties in microphysical parameterizations within NWP models [38] and [39]; advancements in data assimilation techniques using radar and remote sensing [40]; development of integrated forecasting systems for TC rainfall prediction [41]; and improvements in ground-based radar, airborne radar, and satellite technologies for observing TC rainfall. In addition, advances in ground-based radar, airborne radar, and satellite observations have greatly improved rainfall observation. Despite these advances, ongoing challenges in tropical cyclone rainfall forecasting remain, including difficulties in monitoring rainfall, inherent variability, and complex synoptic conditions during landfall [19].

In 2008, the accuracy of the ECMWF-IFS model in forecasting the tracks of medium-scale tropical cyclones was evaluated using the IFS model [42]. Over the study period, the model's forecast accuracy for cyclone tracks improved significantly. Forecasts based on consensus (consensus, or simple averaging) demonstrated higher accuracy than individual forecasts (typically 20% better for 72-hour lead times). Forecast accuracy was also improved by improvements in convective parameterization.

As well as assessing forecast accuracy for TC's track and intensity, numerous detailed studies have been conducted [43][44][45][46] and [47]. These studies compared and evaluated the accuracy of global models in predicting TC's track and intensity. Researchers used new analysis methods such as the Track Error Rose (TER) and Taylor diagrams to

analyze forecast errors compared to observed TCs in their 2013, 2015, and 2021 studies. According to evaluation results, the ECMWF model performs relatively well compared to other models, and the accuracy of TC's track forecasting has improved significantly in recent years, though TC's intensity forecasting has not improved significantly.

Based on a 24-hour lead time for two global models, GFS and ECMWF, the track and intensity forecasts of Typhoon Dineo, which made landfall in southern Mozambique on February 15, 2017, were analyzed. The analysis indicated that both models produced intensity forecast errors exceeding 17 mb and track forecast errors of approximately 1.4 km or less. Additionally, ECMWF was found to outperform GFS in predicting both the position and intensity of the TC [48]. In accordance with Vietnam's regulatory framework for the evaluation of meteorological and hydrological forecasting and warning quality [49], the technical process for forecasting and warning sets accuracy standards as follows:

- Position of tropical depression center: Reliable within a lead time of 12 hours if forecast error is less than 100 km, within a lead time of 24 hours if forecast error is less than 150 km, and within a lead time of 48 hours if forecast error is less than 200 km.
- TC and tropical depression intensity: Reliable for a lead time of 12 hours when the forecast error is nowhere near 1 level, within a lead time of 24 hours when the forecast error is 1 to 2 levels, and within a lead time of 48 hours when the forecast error is 2 levels.
- The quality of heavy rainfall forecasts is assessed based on specific rainfall classes for a lead time of 48 hours. When the predicted total rainfall is 51-100 mm, observed rainfall between 30 and 150 mm is considered reliable.

While the above studies demonstrate the applicability of the IFS model in forecasting TC track and intensity, important research gaps remain concerning its performance in simulating storm-related rainfall and in evaluating forecast errors against Vietnam's regulatory standards. This study analyzes and evaluates the errors of the IFS model in forecasting TC in Vietnam by using previously used methods for evaluating TC track, intensity, and rainfall forecasting. The study will provide insights and conclusions on the applicability of the IFS model to Vietnam's TC forecasting operations.

## 2. Data and Method

### 2.1 Data

#### 2.1.1 Observed data

The TC's best track data in 2018-2022 period can be download from RSMC: <https://www.jma.go.jp/jma/jma-eng/jma-center/rsmc-hp-pub-eg/besttrack.html> including the information of location (LAT, LONG) of TCs, maximum wind speed ( $V_{max}$ ), minimum pressure at center ( $P_{min}$ ) and 6 hourly temporal resolution. The research domain is defined as 5°N - 25°N and 100°E - 125°E. Figure 1 shows the TCs track and intensity by knots during the period from 2018 to 2022. Analyze this data, there were about 37 TCs affecting the South China Sea and Vietnam, of these 24 TCs in landfall and coastal Vietnam. There are 186 synoptic stations of Vietnam are represented by dots based on observations made around the same time.

In this study, IFS model's forecast products from 2018-2022 period with a horizontal resolution of about 9 km were used, the spatial resolution of the data is  $0.125 \times 0.125^\circ$ , detailed descriptions are given in <https://www.ecmwf.int/en/forecasts/documentation-and-support/changes-ecmwf-mode>. The IFS model is a global numerical weather prediction system. It represents atmospheric motions across all spatial and temporal scales. The IFS framework consists of two main components: (i) the atmospheric general circulation model, which is coupled with the ocean wave model, the ocean general circulation model,

and the land surface model; and (ii) the four-dimensional variational (4DVAR) data assimilation system. IFS products are available at above website, where the ECMWF provides deterministic IFS outputs in both numerical (GRIB2) and graphical formats. The NCHMF of Vietnam receives deterministic medium-range forecasts from the IFS model at a horizontal resolution of 9 km, twice daily (00UTC and 12UTC). The products available on the ECMWF website are predefined for different regions, accessible for visualization only, and cannot be modified. Furthermore, access to these products requires a registered user account. At the NCHMF of Vietnam, the IFS datasets are decoded into relevant meteorological variables and subsequently distributed to end users in both graphical and numerical formats. For TC forecasts, the data are presented in both numerical and graphical formats, including track, intensity, and precipitation forecasts at 6-hour intervals up to 72 hours from the IFS model outputs.

#### 2.1.2 Products of IFS model

In this study, IFS model's forecast products from 2018-2022 period with a horizontal resolution of about 9 km were used, the spatial resolution of the data is  $0.125 \times 0.125^\circ$ , detailed descriptions are given in <https://www.ecmwf.int/en/forecasts/documentation-and-support/changes-ecmwf-mode>.

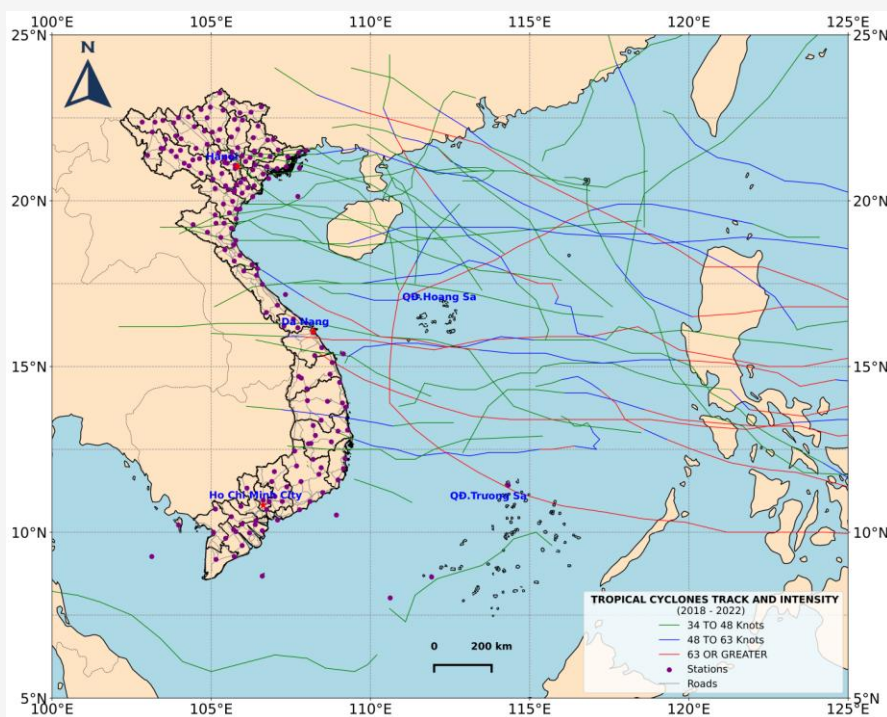


**Figure 1:** TC's best track and intensity in 2018-2022

The IFS model is a global numerical weather prediction system. It represents atmospheric motions across all spatial and temporal scales. The IFS framework consists of two main components: (i) the atmospheric general circulation model, which is coupled with the ocean wave model, the ocean general circulation model, and the land surface model; and (ii) the four-dimensional variational (4DVAR) data assimilation system. IFS products are available at above website, where the ECMWF provides deterministic IFS outputs in both numerical (GRIB2) and graphical formats. The NCHMF of Vietnam receives deterministic medium-range forecasts from the IFS model at a horizontal resolution of 9 km, twice daily (00UTC and 12UTC). The products available on the ECMWF website are predefined for different regions, accessible for visualization only, and cannot be modified. Furthermore, access to these products requires a registered user account. At the NCHMF of Vietnam, the IFS datasets are decoded into relevant meteorological variables and subsequently distributed to end users in both graphical and numerical formats. For TC forecasts, the data are presented in both numerical and graphical formats, including track, intensity, and precipitation forecasts at 6-hour intervals up to 72 hours from the IFS model outputs.

## 2.2 Verification Methodology

The conceptual framework of this study is shown in Figure 2, where input data is taken from the IFS model, the best track of TC from RSMC, and rainfall observed; the data is then processed, statistic matrices are obtained, and the final results are verification indices. To evaluate the spatial accuracy of the forecasted track, the Direct Positional Error

(*DPE*) was employed as a geodetic metric quantifying the separation between the forecast and observed cyclone centers. Unlike *MAE* and *RMSE*, which assess discrepancies in scalar variables, *DPE* captures both the magnitude and directional components of positional error, making it particularly suitable for trajectory-based verification. Positional error metrics such as *DPE* are widely used to assess TC track performance in numerical weather prediction systems, including those of the Met Office [50]. In an analysis of TC forecasts in the Western North Pacific, the average *DPE* at 24, 48, 72, 96, and 120 hour lead times was reported to be on the order of 80–400 km, depending on the forecast model [51]. Furthermore, other studies in extratropical contexts also compute *DPE* alongside cross-track error (CTE) and along-track error (ATE) for a more detailed bias decomposition [52].

In this study, the *DPE* (in km) is used as the verification metric to analyze the track forecast performance of the IFS model. *DPE* is defined as the great-circle distance between the observed (best track) position and the forecasted position, and was used by [51] [53] and [54]. Following the equation commonly adopted in the literature, the *DPE* is calculated in Equation 1.

$$DPE = R \cdot \cos^{-1} \left[ \begin{array}{l} \sin(X_o) \sin(X_f) \\ + \cos(X_o) \cos(X_f) \cos(Y_f - Y_o) \end{array} \right] \quad \text{Equation 1}$$

Where *R* is the mean radius of the Earth ( $\approx 6,371$  km), *X* denotes latitude, *Y* denotes longitude, and the subscripts “*o*” and “*f*” refer to observed and forecasted positions, respectively.

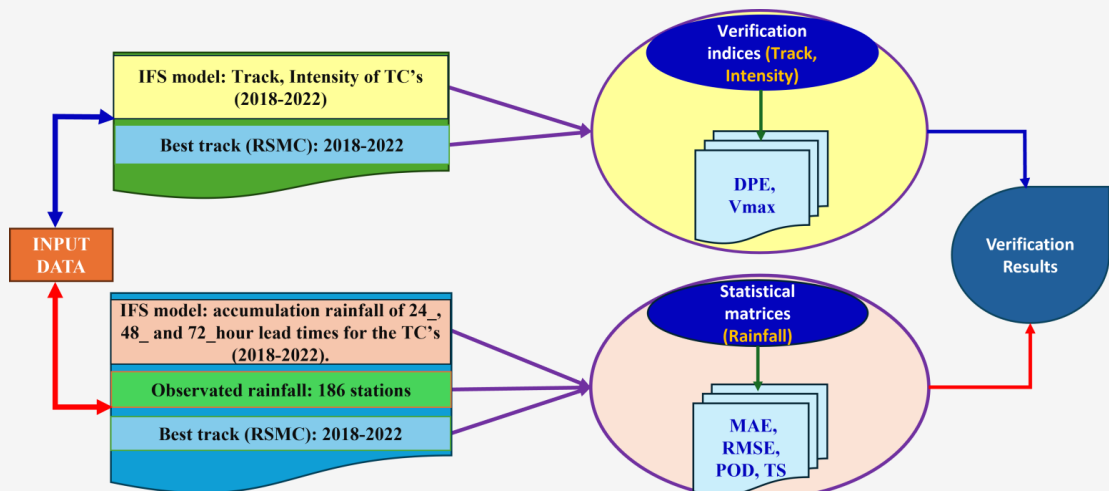


**Figure 2:** Conceptual framework of the applied methodology in this study

The intensity of the TC is taken from the maximum wind speed ( $V_{max}$ ) at the center of the TC and evaluated through the *MAE* (mean absolute error) and *RMSE* (square root of the mean square error) indices. The use of *MAE* and *RMSE* follows common practice in tropical cyclone verification, as both metrics provide quantitative measures of forecast accuracy for continuous variables such as maximum sustained wind speed. *MAE* represents the average magnitude of forecast errors and is insensitive to outliers, thus offering a robust estimate of typical forecast performance. In contrast, *RMSE* places greater weight on larger deviations and is therefore effective in identifying cases of substantial forecast failure. The utility of these metrics has been widely demonstrated in previous studies: For the evaluation of TC intensity forecasts, *MAE* and *RMSE* were employed, and these metrics were likewise adopted to quantify errors in model-based TC intensity predictions [55]. *MAE* and *RMSE* are calculated in Equation 2 and Equation 3.

$$MAE = \frac{1}{N} \sum_{i=1}^N |f_i - o_i|$$

Equation 2

$$RMSE = \sqrt{\frac{1}{N} \sum_{i=1}^N (f_i - o_i)^2}$$

Equation 3

Where  $N$  is the sample size,  $f_i$  denotes the predicted value, and  $o_i$  denotes the observed value.

The TC size is determined based on [56], so TC's rainfall was calculated from its center to a radius of

500 km by using the TC's best track for the station rainfall and the forecast rainfall. Based on the station rainfall and the forecast rainfall, we compared the *MAE*, *RMSE*, *TS* (threat score) and *POD* (probability of detection) indices [57]. *TS* and *POD* are calculated in Equation 4 and Equation 5.

$$TS = \frac{H}{H + M + F}$$

Equation 4

$$POD = \frac{H}{H + M}$$

Equation 5

Where  $H$  denotes Hits,  $M$  denotes Misses, and  $F$  denotes False Alarms. A Hit refers to an event that was correctly forecast and subsequently observed, meaning the model successfully predicted the occurrence of the event. A Miss corresponds to an event that was not forecast but did occur, indicating that the model failed to capture an observed event. A False Alarm refers to an event that was forecast to occur but did not actually take place, representing an incorrect prediction of an event that never happened. The *TS* ranges from 0 to 1, where 0 indicates no skill and 1 represents a perfect forecast. Similarly, the *POD* ranges from 0 to 1, with a value of 1 indicating perfect detection of all observed events.

### 3. Results and Discussion

#### 3.1 The Tropical Cyclone Track

Figure 3 illustrates the *DPE* values for the period 2018–2022 at 24-hour, 48-hour, and 72-hour lead times, corresponding to 220, 155, and 102 forecast cases, respectively.

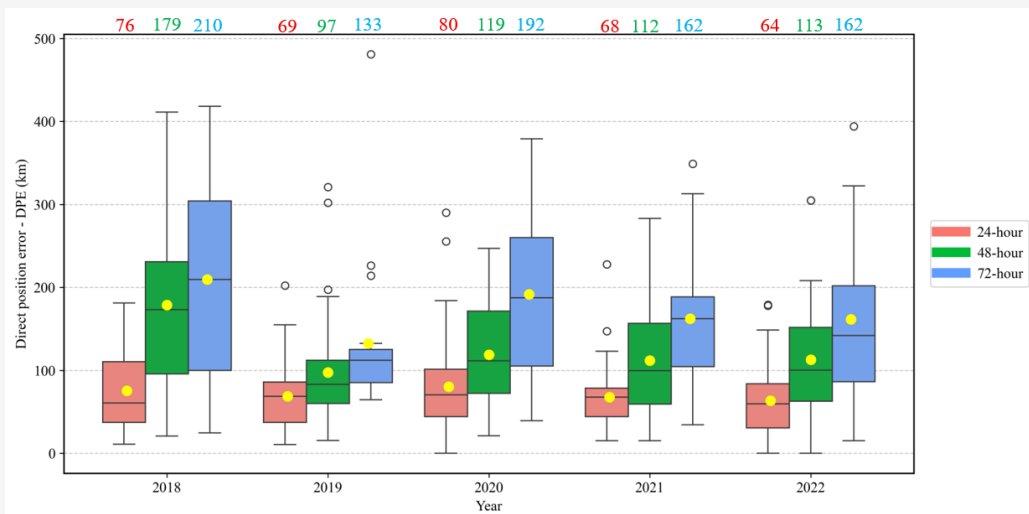


**Figure 3:** Evaluation of the IFS model using the *DPE* index for 24-hour, 48-hour, 72-hour lead times from 2018–2022 (black bars represent median values; yellow dots represent mean values)

The mean values increase steadily from 71 km (24-hour lead time) to 118 km (48-hour lead time), reaching 183 km (72-hour lead time). This pattern indicates a systematic growth in forecast errors as the lead time increases, which is consistent with the well-established characteristic of numerical weather prediction models where forecast accuracy decreases over longer lead times. The median values follow a similar upward trend, suggesting a uniform shift of the error distribution toward higher levels. In terms of dispersion, standard deviation show a sharp increase with forecast length: from 46 km (24-hour lead time) to 72 km (48-hour lead time), and reaching

146 km at 72-hour lead time. This implies not only a rise in mean error but also greater variability of errors over longer horizons. However, when compared with the regulatory framework of Vietnam, these values fall within the permissible error classes for TC forecasting and warning, thereby demonstrating that the IFS model meets the national requirements for operational use. This suggests that the IFS model provides sufficiently accurate track forecasts to support official TC warning operations in Vietnam. We also applied the Mann–Kendall test to detect trends in *DPE* (Figure 4).

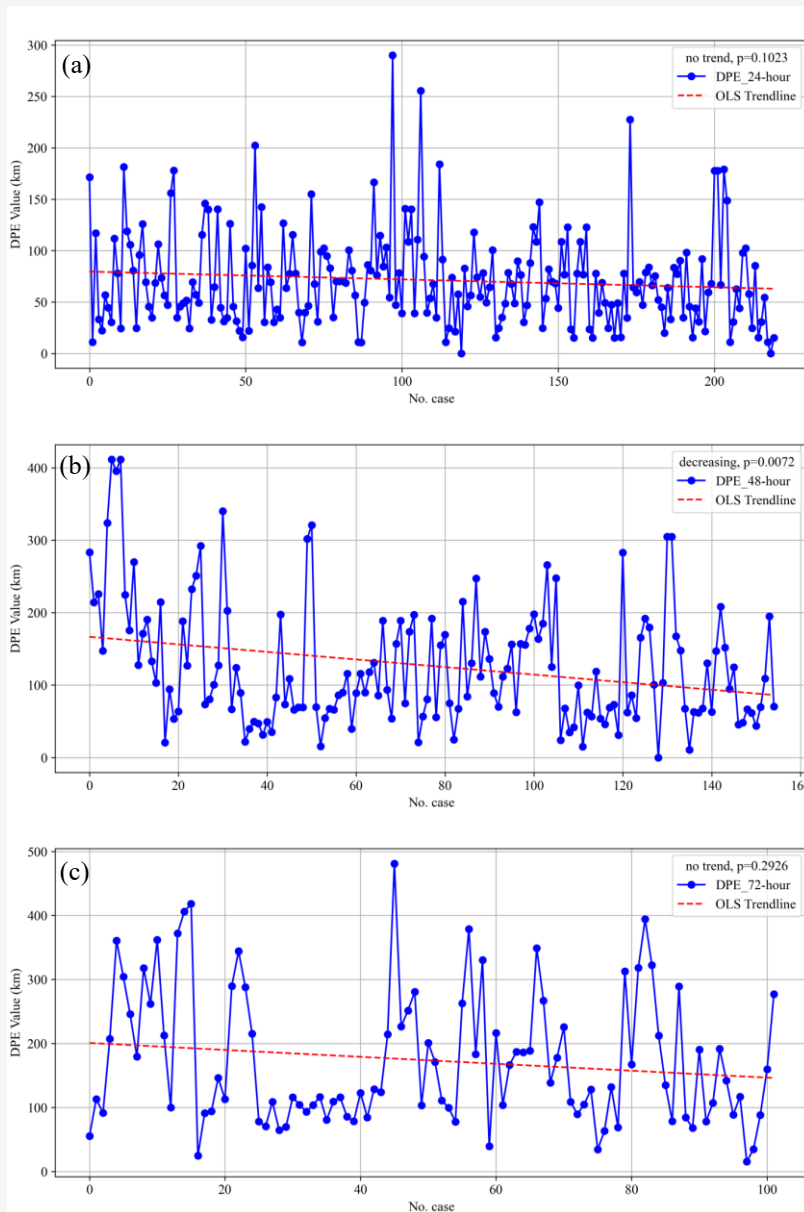


**Figure 4:** Mann–Kendall test results for trends in *DPE* from 2018-2022: (a) 24-hour, (b) 48-hour, and (c) 72-hour lead times

No significant trend was identified for the 24-hour and 72-hour lead times, whereas the 48-hour lead time exhibited a decreasing trend in  $DPE$ , with a  $p$ -value of approximately 0.0072, indicating a statistically significant downward trend at the 1% significance level. Thus, the absence of significant trends at 24-hour and 72-hour lead times suggests stable error behavior, while the significant downward trend at the 48-hour horizon reflects a gradual improvement in model accuracy for this lead time.

### 3.2 Tropical Cyclone Intensity

Figure 5 present the  $MAE$  and  $RMSE$  indices of  $V_{max}$  at 24-hour, 48-hour, and 72-hour lead times during 2018–2022, corresponding to 178, 100, and 59 forecast cases, respectively. The statistical evaluation of the  $MAE$  of  $V_{max}$  at 24-hour, 48-hour, and 72-hour lead times demonstrates a relatively stable level of forecast accuracy across different horizons. The mean errors remain close to 9 knots throughout (corresponding to roughly 4.63 m/s), with the highest at 24-hour (9.3 knots), the lowest at 48-hour (8.9 knots), and a slight increase again at 72-hour (9.1 knots). Similarly, the  $RMSE$  of  $V_{max}$  fluctuates slightly but generally centers around 12 knots (corresponding to roughly 6.17 m/s) across the lead times. These small differences suggest that the forecasting system maintains stable accuracy within the 3-day forecast horizon. Compared with the regulatory framework of Vietnam, the mean results fall within the allowable error thresholds for  $V_{max}$  in tropical cyclone forecasts. However, individual cases with exceptionally large forecast errors reduce the overall reliability of predictions. A notable example

is Typhoon RAI (2122), which developed on 16 December 2021 and dissipated on 21 December 2021. For this event, the 72-hour forecast  $RMSE$  of  $V_{max}$  reached 30–40 knots, the largest error recorded in the study period. This anomaly was attributable to RAI's rapid and extreme intensity fluctuations. Originating as a tropical depression over the northwestern Pacific, RAI intensified into a super typhoon within three days. After crossing the Philippines, it weakened into a very strong typhoon before re-intensifying into a super typhoon over the South China Sea. Remarkably, RAI was the first super typhoon observed in the South China Sea since 1961. During its development stage, the numerical weather prediction model systematically underestimated its intensity [58].

### 3.3. Tropical Cyclone Rainfall

In accordance with Vietnam's legal framework on rainfall classification [49], rainfall is categorized as follows:

- Light rain: less than 16 millimeters,
- Moderate rain: from over 16 millimeters up to 50 millimeters
- Heavy rain: more than 50 millimeters up to 100 millimeters
- Very heavy ran: over 100 millimeters

In this study, statistical indices were calculated using these rainfall classes. Observed rainfall data from 186 stations resulted in approximately 104 analyzed cases.

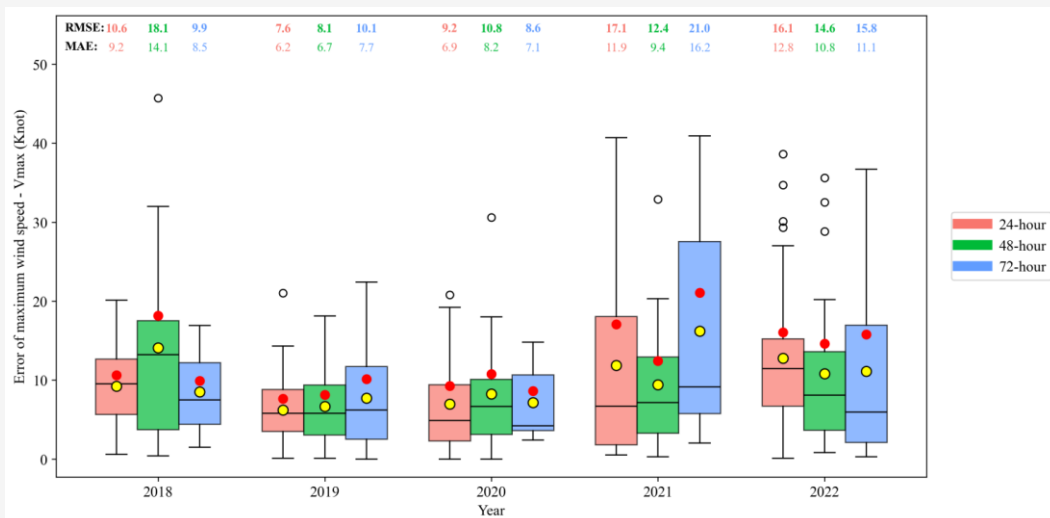


**Figure 5:** Evaluation of the IFS model using  $MAE$  index by  $V_{max}$  for 24-hour, 48-hour, 72-hour lead times from 2018–2022 (black bars represent median values; yellow dots represent mean value of  $MAE$  of  $V_{max}$ ; red dots represent mean value of  $RMSE$  of  $V_{max}$ )

### 3.3.1 24-hour lead time

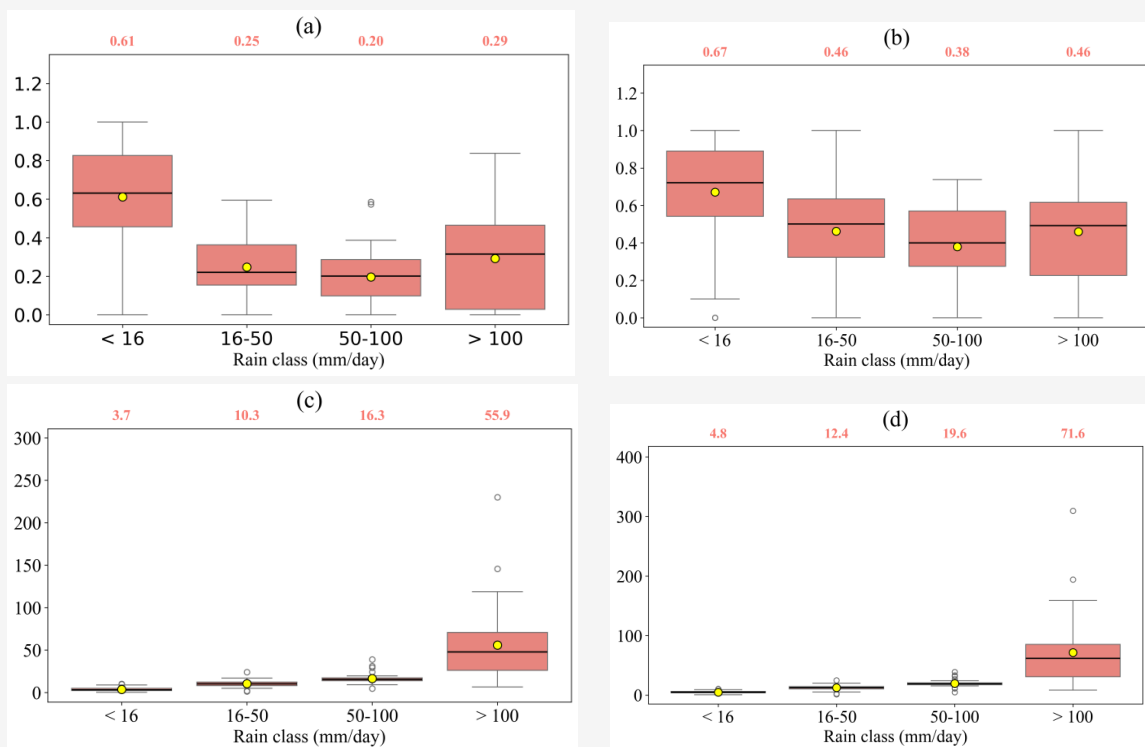
For the 24-hour lead time during the period 2018–2022, Figure 6 presents the statistical indices including *TS*, *POD*, *MAE*, and *RMSE* across different rainfall classes. For a given class, higher *TS* and *POD* values indicate better forecast performance. Specifically, for rainfall below 16 mm, the mean *TS* and *POD* are 0.61 and 0.67, respectively. This is followed by the 16–50 mm and above 100 mm classes, which yield relatively similar results, with mean *TS* ranging from 0.25 to 0.29 and mean *POD* consistently at 0.46. The 50–100 mm class shows the lowest mean *TS* and *POD* values, at 0.20 and 0.38, respectively. Clearly, the IFS model demonstrates the highest skill in forecasting rainfall events below 16 mm compared with other classes, with the correct detection rate reaching approximately 70%. For the remaining classes, the detection rate is relatively similar, at around 40–50%. For rainfall below 16 mm, the mean *RMSE* is approximately 5 mm/day, while the mean *RMSE* values for the 16–50 mm and 50–100 mm classes are 12 mm/day and 20 mm/day, respectively. For rainfall above 100 mm, the mean *RMSE* is about 72 mm/day, with maximum values reaching up to 300 mm/day in certain cases.

Figure 7 illustrates the spatial distribution of *MAE* across different regions of Vietnam according

to rainfall classes within the 24-hour lead time. For rainfall amounts below 16 mm, higher *MAE* values are observed in the western part of Northern Vietnam, as well as in Central and Southern Vietnam. For the 16–50 mm class, *MAE* is more uniformly distributed across the country. In the 50–100 mm range, higher *MAE* values are concentrated in the Red River Delta and Central Vietnam. For rainfall amounts exceeding 100 mm, the spatial pattern of higher *MAE* is generally similar to that observed in the 50–100 mm class.

### 3.3.2 48-hour lead time

Figure 8 presents the statistical indices including *TS*, *POD*, *MAE*, and *RMSE* across different rainfall classes for the 48-hour forecast lead time. The highest *TS* and *POD* values are observed for rainfall below 16 mm, with means of 0.67 and 0.77, respectively, and these values decrease with increasing rainfall classes, reaching the lowest levels for rainfall above 100 mm (0.10 and 0.17, respectively). The highest correct detection rate is associated with rainfall below 16 mm, reaching up to 80%. For the 16–50 mm and 50–100 mm classes, the correct detection rates are approximately 40% and 30%, respectively. The lowest detection rate is observed for rainfall above 100 mm, at around 20%.



**Figure 6:** Evaluations of the IFS model using statistical indices by rainfall classes (black bar is median value; yellow dot is mean value) for 24-hour lead time from 2018–2022: (a) *TS*, (b) *POD*, (c) *MAE*, and (d) *RMSE*

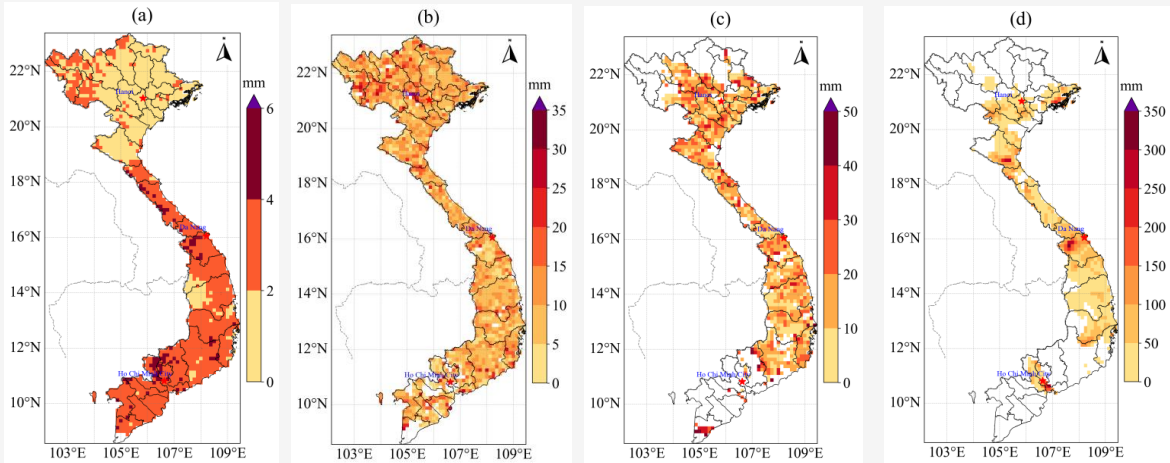


**Figure 7:** The spatial distribution of *MAE* index across different regions of Vietnam for the 24-hour lead time according to rainfall classes:

(a) less than 16 mm, (b) 16–50 mm, (c) 50–100 mm, and (d) greater than 100 mm

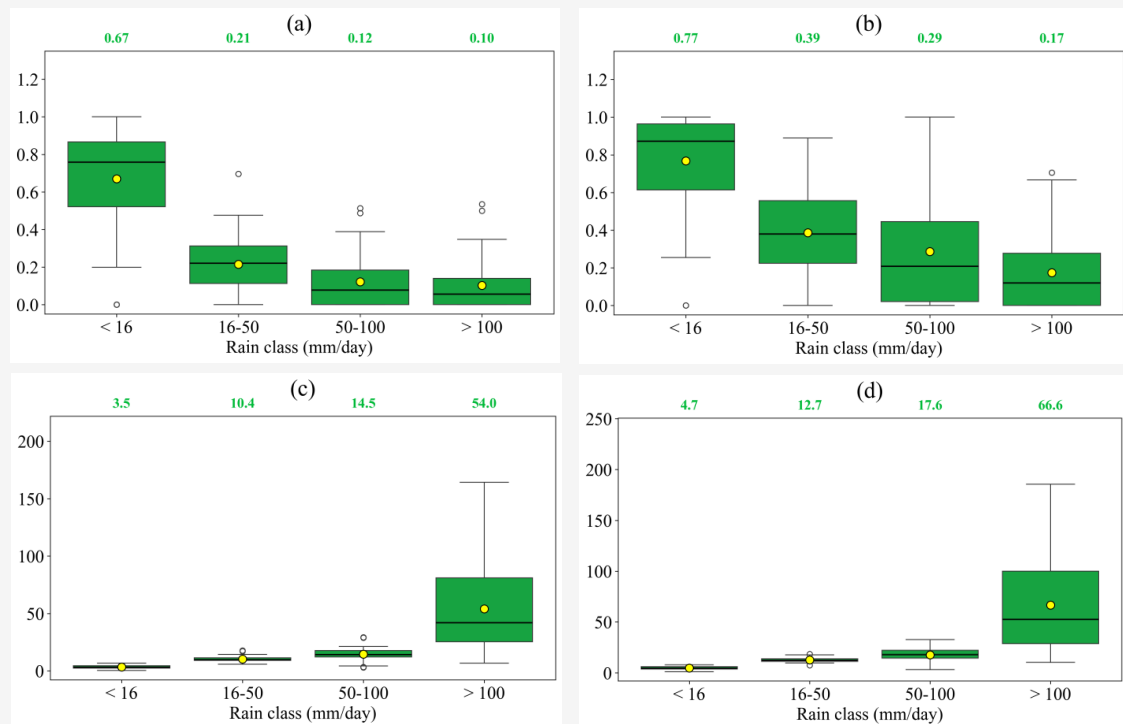


**Figure 8:** Evaluations of the IFS model using statistical indices by rainfall classes (black bar is median value; yellow dot is mean value) for 48-hour lead time from 2018–2022: (a) *TS*, (b) *POD*, (c) *MAE*, and (d) *RMSE*

For rainfall below 16 mm, the mean *RMSE* is approximately 5 mm/day, while for the 16–50 mm and 50–100 mm classes, the mean *RMSE* values are 13 mm/day and 18 mm/day, respectively. For rainfall above 100 mm, the mean *RMSE* is about 67 mm/day, with maximum values reaching up to 190 mm/day in certain cases. The spatial distribution of *MAE* across different regions of Vietnam according to rainfall classes for the 48-hour lead time exhibits a similar

pattern to that of the 24-hour lead time and is presented in Figure 9.

### 3.3.3 72-hour lead time

Similarly, the statistical indices across rainfall classes for the 72-hour forecast lead time are presented in Figure 10. The highest mean *TS* and *POD* values are observed for rainfall below 16 mm, at 0.74 and 0.85, respectively.

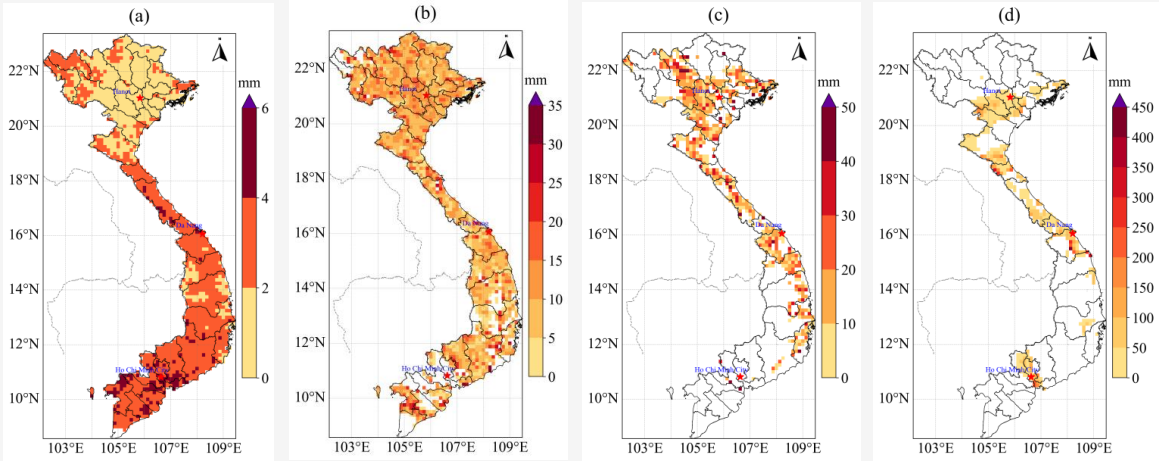


**Figure 9:** The spatial distribution of *MAE* index across different regions of Vietnam for the 48-hour lead time according to rainfall classes: (a) less than 16 mm, (b) 16–50 mm, (c) 50–100 mm, and (d) greater than 100 mm

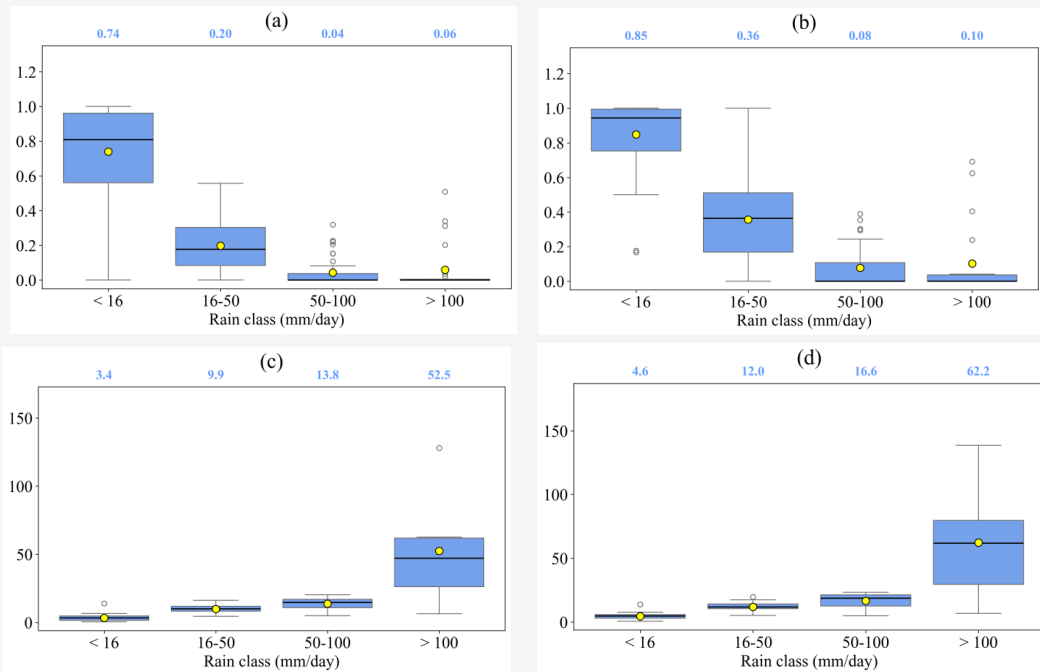


**Figure 10:** Evaluations of the IFS model using statistical indices by rainfall classes (black bar is median value; yellow dot is mean value) for lead time 72-hour from 2018–2022: (a) *TS*, (b) *POD*, (c) *MAE*, and (d) *RMSE*

For the 16–50 mm class, the mean *TS* and *POD* values decrease but still reach 0.20 and 0.36, respectively. For the 50–100 mm and above 100 mm classes, the mean *TS* and *POD* values decline rapidly, with *TS* below 0.06 and *POD* below 0.10. This indicates that the model’s skill in forecasting heavy to very heavy rainfall at the 72-hour lead time is significantly lower than for the other rainfall classes and also lower compared with the 24-hour and 48-hour lead times. For rainfall below 16 mm, the mean

*RMSE* is approximately 5 mm/day, while for the 16–50 mm and 50–100 mm classes, the mean *RMSE* values are 12 mm/day and 17 mm/day, respectively. For rainfall above 100 mm, the mean *RMSE* reaches the highest value of about 62 mm/day, with maximum values up to 139 mm/day in certain cases. For the 72-hour lead time, the spatial distribution of *MAE* across regions of Vietnam shows some differences compared to the 24-hour and 48-hour lead times (Figure 11).

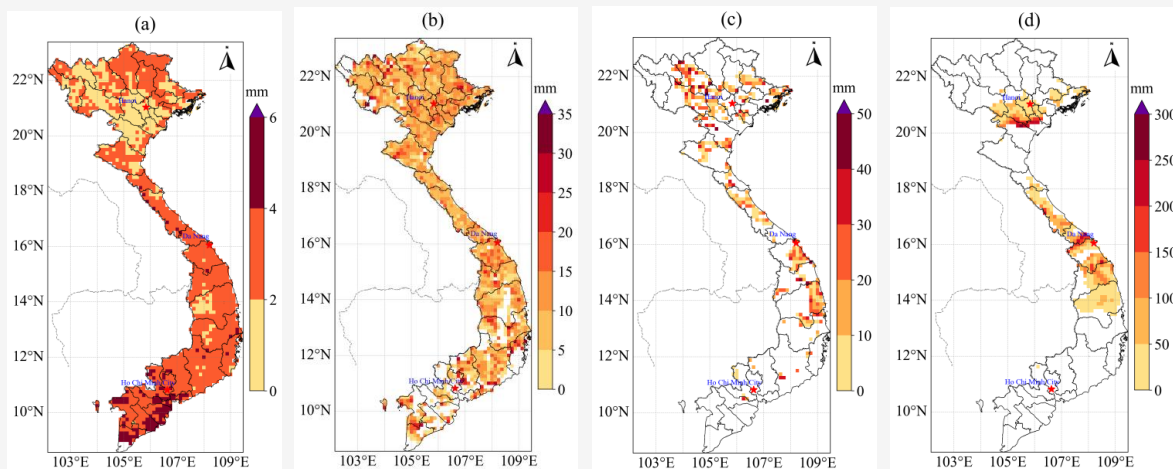


**Figure 11:** The spatial distribution of *MAE* index across different regions of Vietnam for the 72-hour lead time according to rainfall classes: (a) less than 16 mm, (b) 16–50 mm, (c) 50–100 mm, and (d) greater than 100 mm

For rainfall amounts below 16 mm, higher *MAE* values are observed in the northern mountainous areas, Central Vietnam, and Southern Vietnam, with particularly pronounced values in the South. For the 16–50 mm class, higher *MAE* values are concentrated in Northern and Central Vietnam. In the 50–100 mm class, elevated *MAE* values are unevenly distributed, appearing sporadically in the Red River Delta and Central Vietnam. For rainfall amounts exceeding 100 mm, higher *MAE* values are mainly distributed over the Red River Delta and the central to southern parts of Central Vietnam.

#### 4. Conclusions

This study evaluates the accuracy of the IFS model by comparing its forecast products for 2018–2022 with best track data from the RSMC and rainfall observations from 186 stations in Vietnam, for 24-hour, 48-hour, 72-hour lead times. Also, these statistical indices were compared with Vietnamese assessment regulations, resulting in the following results:

For the TC track forecasts, the mean *DPE* increases with lead time, from 71 km (24-hour lead time) to 118 km (48-hour lead time) and 183 km (72-hour lead time), with greater variability at longer horizons. Nevertheless, these values remain within Vietnam's permissible thresholds, confirming that the IFS model meets operational requirements. Notably, the Mann–Kendall test reveals a significant downward trend at the 48-hour lead time (*p*-value of approximately 0.0072), reflecting improved forecast accuracy during the study period.

For TC intensity forecasts, errors varied little across the forecast lead times, with the mean *MAE* of  $V_{max}$  approximately 9 knots (4.63 m/s) and the mean *RMSE* of  $V_{max}$  about 12 knots (6.17 m/s), both within Vietnam's permissible thresholds. However, exceptional cases such as Typhoon RAI (2021) demonstrated that errors can increase substantially (with *RMSE* of  $V_{max}$  reaching 30–40 knots), highlighting the challenges of predicting rapid and extreme intensity changes. This underscores the necessity of improving models and applying post-processing techniques to enhance the reliability of early warnings for severe tropical cyclones in Vietnam.

For TC rainfall, for rainfall below 16 mm, the IFS model exhibits the highest and most stable skill across all three lead times, as indicated by consistently superior *TS* and *POD* values compared with other classes. This demonstrates the model's ability to maintain and even improve accuracy when forecasting light rainfall events. In contrast, for moderate to very heavy rainfall classes, forecast skill decreases markedly with increasing lead time. At the 16–50 mm class, *TS* and *POD* gradually decline but remain at moderate levels (40% at the 48-hour lead time and 36% at the 72-hour lead time). However, at the 50–100 mm and above 100 mm classes, both *TS* and *POD* values drop sharply, particularly at the 72-hour lead time, where *TS* falls below 0.06 and *POD* below 0.10, indicating substantial limitations in forecasting heavy to very heavy rainfall. Forecasting heavy rainfall at the 72-hour lead time remains a challenge for numerical weather prediction models.

## Acknowledgements

This study was supported by the project titled “Research the scientific basis to develop national technical regulations on assessment of hydro-meteorological forecasting and warning in accordance with the regulations of the World Meteorological Organization (WMO)”. The project was funded under Grant No. TNMT.2023.02.34.

## References

- [1] IMHEN, and UNDP. (2015). Viet Nam Special Report on Managing the Risk of Extreme Events and Disasters to Advance Climate Change Adaptation. *Viet Nam Publishing House of Natural Resources, Environment and Cartography*, Ha Noi, Viet Nam.
- [2] Takagi, H., (2019). Statistics on Typhoon Landfalls in Vietnam: Can Recent Increases in Economic Damage Be Attributed to Storm Trends? *Urban Climate*, Vol. 30. <https://doi.org/10.1016/j.uclim.2019.100506>.
- [3] UNDP Vietnam. (2024). Vietnam – Multi-Sector Assessment (VMSA) Report for Typhoon Yagi Recovery – Impact Report. [Online]. Available: <https://www.undp.org/vietnam/publications/viet-nam-multi-sector-assessment-vmsa-report-typhoon-yagi-recovery> [Accessed: Nov. 30, 2024].
- [4] Vo, H. V., Mai, H. K., Du, T. D. Hole, L. R>, Dinh, Q. D., Anh, D. C., Thi, H. P., and Gia, N. H. (2024). Performance of International Global Models and Official Tropical Cyclone Forecasts Over the Bien Dong Sea for the Period 2012–2019. *Advances In Meteorology*, Vol. 2024(1). <https://doi.org/10.1155/2024/7244738>.
- [5] Ba, T. D., Vo, V. H. and Tri, D. Q., (2019). A Verification of Short-Term Rainfall Forecast by Using IFS Model of ECMWF on the Northern Central Region. *Vietnam Journal of Hydrometeorology*, Vol. 697, 33-43. [https://doi.org/10.36335/VNJHM.2019\(697\).33-43](https://doi.org/10.36335/VNJHM.2019(697).33-43).
- [6] Minh, L. T., Lam, H. P. and Dat, T. T., (2018). Automatically Correction for Forecasts City Temperature from the IFS Model Output. *Vietnam Journal of Hydrometeorology*. Vol. 693, 41-47.
- [7] Hoa, N. N., An, N. L., Tri, D. Q., Dat, T. T., Mai, D. T. and Truong, D. D., (2019). Research on Forecasting and Warning Methods in Hydrometeorological Drought: Case Study at Dak Lak Province, Highland in Vietnam. *Vietnam Journal of Hydrometeorology*. Vol. 699, 31-41.
- [8] Tri, D. Q., (2019). Application Hydrology-Hydraulic Models Combined with Rainfall Forecasting (IFS) in Flood and Inundation Warning on Vu Gia-Thu Bon Basin. *Vietnam Journal of Hydrometeorology*, Vol. 703, 27-41. [https://doi.org/10.36335/VNJHM.2019\(703\).27-41](https://doi.org/10.36335/VNJHM.2019(703).27-41).
- [9] Thai, T. H., Tri, D. Q., Tuyen, T. D. T., Tam, N. T. and Diu, B. T., (2019). Application MIKE SHE Model Combined with Rainfall Forecasting Product (IFS) to Forecast Inflow to Reservoirs on Tra Khuc-Song Ve Basin. *Vietnam Journal of Hydrometeorology*, Vol. 697, 1-12.
- [10] Hue, L. T. and Lan, N. T., (n.d.). *Applying Rain Forecasts from the WRF3KM-IFS-DA Model to Improve the Effectiveness of Urban Flood Forecasting and Warning*. [Online]. Available: [https://doi.org/10.36335/vnjhm.2024\(763\).48-65](https://doi.org/10.36335/vnjhm.2024(763).48-65) [Accessed: Nov. 30, 2024].
- [11] Xe, L. V., Hoa, V. V. and Son, L. T., (2019). A Verification of Heavy Rainfall Events Forecast Accuracy of IFS Model at the Middle Central of Vietnam. *Vietnam Journal of Hydrometeorology*. [https://doi.org/10.36335/VNJHM.2019\(3\).48-55](https://doi.org/10.36335/VNJHM.2019(3).48-55).
- [12] Ha, L. T. T., Hang, N. T., Hai, T. T. T. and Tuyet, N. T., (2024). Evaluate the Correct and the Accuracy of the IFS Model for Minimum Temperature, Average Temperature, Maximum Temperature Forecasting in Short Term (24 Hours) at 09 Regions in Vietnam. *Vietnam Journal of Hydrometeorology*. [https://doi.org/10.36335/vnjhm.2024\(18\).92-104](https://doi.org/10.36335/vnjhm.2024(18).92-104).
- [13] Zhou, F., Yamaguchi, M. and Qin, X., (2016). Possible Sources of Forecast Errors Generated by the Global/Regional Assimilation and Prediction System for Landfalling Tropical Cyclones. Part I: Initial Uncertainties. *Advances In Atmospheric Sciences*, Vol. 33, 841–851. <https://doi.org/10.1007/s00376-016-5238-4>.
- [14] Zhou, F., Duan, W., Zhang, H. and Yamaguchi, M. (2018). Possible Sources of Forecast Errors Generated by the Global/Regional Assimilation and Prediction System for Landfalling Tropical Cyclones. Part II: Model Uncertainty. *Advances In Atmospheric Sciences*, Vol. 35, 1277–1290. <https://doi.org/10.1007/s00376-018-7095-9>.
- [15] Tang, C. K., Chan, J. C. L. and Yamaguchi, M., (2021). Large Tropical Cyclone Track Forecast Errors of Global Numerical Weather Prediction Models in Western North Pacific Basin. *Tropical Cyclone Research and Review*. Vol. 10(3), 151-169. <https://doi.org/10.1016/j.terr.2021.07.001>.

- [16] Lei, L., Li, Y. and Tang, Y., (2024). On The Duration of Tropical Cyclone Rapid Intensification. *Geophysical Research Letters*, Vol. 51. <https://doi.org/10.1029/2024GL108578>.
- [17] Ray, K., Balachandran, S. and Dash, S. K., (2022). Challenges of Forecasting Rainfall Associated with Tropical Cyclones in India. *Meteorology And Atmospheric Physics*, Vol. 134, <https://doi.org/10.1007/s00703-021-00842-w>.
- [18] Lamers, A., Devi, S. S., Sharma, M., Berg, R., Gálvez, J. M. and Yu, Z., (2023). Forecasting Tropical Cyclone Rainfall and Flooding Hazards and Impacts. *Tropical Cyclone Research and Review*, Vol. 12(2), 100-112. <https://doi.org/10.1016/j.tcr.2023.06.005>.
- [19] Cheung, K., Yu, Z., Elsberry, R. L., Bell, M., Jiang, H., Lee, T. C., Lu, K., Oikawa, Y., Qi, L., Rogers, R. F. and Tsuboki, K., (2018). Recent Advances in Research and Forecasting of Tropical Cyclone Rainfall. *Tropical Cyclone Research and Review*, Vol. 7(2), 106-127. <https://doi.org/10.6057/2018TCRR02.03>.
- [20] Bao, X., Davidson, N. E., Yu, H., Hankinson, M. C. N., Sun, Z., Rikus, L. J., Liu, J., Yu, Z. and Wu, D., (2015). Diagnostics for an Extreme Rain Event Near Shanghai During the Landfall of Typhoon Fitow (2013). *Monthly Weather Review*, Vol. 143, 3377-3405. <https://doi.org/10.1175/MWR-D-14-00241.1>.
- [21] Deng, D., Davidson, N. E., Hu, L., Tory, K. J., Hankinson, M. C. N. and Gao, S., (2017). Potential Vorticity Perspective of Vortex Structure Changes of Tropical Cyclone Bilis (2006) during a Heavy Rain Event Following Landfall. *Monthly Weather Review*, Vol. 145, 1875-1895. <https://doi.org/10.1175/MWR-D-16-0276.1>.
- [22] Tang, X., Lee, W. C. and Bell, M., (2014). A Squall-Line-Like Principal Rainband in Typhoon Hagupit (2008) Observed by Airborne Doppler Radar. *Journal of Atmospheric Sciences*, Vol. 71, 2733-2746. <https://doi.org/10.1175/JAS-D-13-0307.1>.
- [23] Wang, C. C., Kuo, H. C., Johnson, R. H., Lee, C. Y., Huang, S. Y. and Chen, Y. H., (2015). A Numerical Study of Convection in Rainbands of Typhoon Morakot (2009) with Extreme Rainfall: Roles of Pressure Perturbations with Low-Level Wind Maxima. *Atmospheric Chemistry and Physics*, Vol. 15, 11097-11115.
- [24] Galarneau, T. J., (2015). Influence of a Predecessor Rain Event on the Track of Tropical Cyclone Isaac (2012). *Monthly Weather Review*, Vol. 143, 3354-3376. <https://doi.org/10.1175/MWR-D-15-0053.1>.
- [25] Bell, M. M., (2017). Extreme Precipitation from Tropical Cyclones, Invited Review at the Sixth International Workshop on Monsoons (IWM-VI). *World Meteorological Organization, Singapore*; 13-17 November.
- [26] Yu, Z., Wang, Y. and Xu, H., (2015). Observed Rainfall Asymmetry in Tropical Cyclones Making Landfall Over China. *Journal of Applied Meteorology and Climatology*, Vol. 54, 117-136.
- [27] DeHart, J. C. and Houze, R. A., (2017). Orographic Modification of Precipitation Processes in Hurricane Karl (2010). *Monthly Weather Review*, Vol. 145(10), 4171-4186. <https://doi.org/10.1175/MWR-D-17-0014.1>.
- [28] Yu, Z., Wang, Y., Xu, H., Davidson, N. E., Chen, Y., Chen, Y. and Yu, H., (2017). On the Relationship between Intensity and Rainfall Distribution in Tropical Cyclones Making Landfall Over China. *Journal Of Applied Meteorology and Climatology*, Vol. 56, 2883-2901. <https://doi.org/10.1175/JAMC-D-16-0334.1>.
- [29] Rogers, R. F., Reasor, R. D. and Zhang, J. A., (2015). Multiscale Structure and Evolution of Hurricane Earl (2010) during Rapid Intensification. *Monthly Weather Review*, Vol. 143, 536-562. <https://doi.org/10.1175/MWR-D-14-00175.1>.
- [30] Susca-Lopata, G., Zawislak, J., Zipser, E. J. and Rogers, R. F., (2015). The Role of Observed Environmental Conditions and Precipitation Evolution in the Rapid Intensification of Hurricane Earl (2010). *Monthly Weather Review*, Vol. 143, 2207-2223. <https://doi.org/10.1175/MWR-D-14-00283.1>.
- [31] Zawislak, J., Jiang, H., Alvey, G. R. III, Zipser, E. J., Rogers, R. F., Zhang, J. A. and Stevenson, S. N., (2016). Observations of the Structure and Evolution of Hurricane Edouard (2014) during Intensity Change. Part I: Relationship between the Thermo-Dynamic Structure and Precipitation. *Monthly Weather Review*, Vol. 144, 3333-3354. <https://doi.org/10.1175/MWR-D-16-0018.1>.
- [32] Rogers, R. F., Zhang, J. A., Zawislak, J., Jiang, H., Alvey, G. R. III, Zipser, E. J. and Stevenson, S. N., (2016). Observations of the Structure and Evolution of Hurricane Edouard (2014) during Intensity Change. Part II: Kinematic Structure and the Distribution of Deep Convection. *Monthly Weather Review*, Vol. 144, 3355-3376.

- [33] Nguyen, L. T., Rogers, R. F. and Reasor, P. D. (2017). Thermodynamic And Kinematic Influences on Precipitation Symmetry in Sheared Tropical Cyclones: Bertha and Cristobal (2014). *Monthly Weather Review*, Vol. 135, 4423-4446. <https://doi.org/10.1175/MWR-D-17-0073.1>.
- [34] Pohl, B., Morel, B., Barthe, C. and Bousquet, O., (2016). Regionalizing Rainfall at Very High Resolution Over La Réunion Island: A Case Study for Tropical Cyclone Ando. *Monthly Weather Review*, Vol. 144, 4081-4099. <https://doi.org/10.1175/MWR-D-15-0404.1>.
- [35] Wang, C. and Zeng, Z., (2018). The Effect of Model Horizontal Resolution on the Precipitation of Rammasun. *Journal of Tropical Meteorology*, Vol. 24, 24-263.
- [36] Tsuboki, K. and Sakakibara, A., (2002). Large Scale Parallel Computing of Cloud Resolving Storm Simulator. High Performance Computing. *Springer*, 243-259. [https://doi.org/10.1007/3-540-47847-7\\_21](https://doi.org/10.1007/3-540-47847-7_21).
- [37] Tsuboki, K., (2008). High-Resolution Simulations of High-Impact Weather Systems Using the Cloud-Resolving Model on the Earth Simulator. In: High Resolution Numerical Modeling of the Atmosphere and Ocean. Kevin Hamilton and Wataru Ohfuchi (Eds.). *Springer*, 141-156.
- [38] Hendricks, E. A., Jin, Y., Moskaitis, J. R., Doyle, J. D., Peng, M. S., Wu, C. C. and Kuo, H. C., (2016). Numerical Simulations of Typhoon Morakot (2009) Using a Multiply Nested Tropical Cyclone Prediction Model. *Weather And Forecasting*, Vol. 31, 627-645. <https://doi.org/10.1175/WAF-D-15-0016.1>.
- [39] Brown, B. R., Bell, M. M. and Frambach, A., (2016). Validation of Simulated Hurricane Drop Size Distributions Using Polarimetric Radar. *Geophysical Research Letters*, Vol. 43. <https://doi.org/10.1002/2015GL067278>.
- [40] Bao, X. and Wu, D., (2017). Improving Extreme Rainfall Forecast of Typhoon Morakot (2009) by Assimilating Radar Data from Taiwan and Mainland China. *Journal Of Meteorological Research*, Vol. 31, 747-766. <https://doi.org/10.1007/s13351-017-6007-8>.
- [41] Hong, J. S., Fong, C. T., Hsiao, L. F., Yu, Y. C. and Tzeng, C. Y., (2015). Ensemble Typhoon Quantitative Precipitation Forecasts Model in Taiwan. *Weather And Forecasting*, Vol. 30, 217-237. <https://doi.org/10.1175/WAF-D-14-00037.1>.
- [42] Fiorino, M., (n.d.). Record-Setting Performance of the ECMWF IFS in Medium-Range Tropical Cyclone. *ECMWF Newsletter*, No. 118, 20-27. <https://doi.org/10.21957/zff5t1zehz>.
- [43] Chen, G., Yu, H. and Cao, Q., (2013). The Performance of Global Models in Track Forecasting over the Western North Pacific from 2010 to 2012. *Tropical Cyclone Research and Review*, Vol. 2(3). <https://doi.org/10.6057/2013TCRR03.02>.
- [44] Chen, G., Yu, H. and Cao, Q., (2015). Evaluation of Tropical Cyclone Forecasts from Operational Global Models over the Western North Pacific in 2013. *Tropical Cyclone Research and Review*, Vol. 4(1), 18-26. <https://doi.org/10.6057/2015TCRR01.03>.
- [45] Chen, G., Tang, J. and Zeng, Z., (2012). Error Analysis on the Forecasts of Tropical Cyclone Over Western North Pacific in 2011. *Meteorological Monthly*, Vol. 38(10), 1238-1246.
- [46] Chen, G., Zhang, X., Yang, M., Yu, H. and Cao, Q., (2021). Performance of Tropical Cyclone Forecasts in the Western North Pacific in 2017. *Tropical Cyclone Research and Review*, Vol. 10(1), 1-15. <https://doi.org/10.1016/j.tcr.2021.03.002>.
- [47] Lei, X. T., Chen, G. M., Zhang, X. P., Chen, P. Y. and Yu, H., (2016). In: Performance of Tropical Cyclone Forecast in Western North Pacific in 2015. *48<sup>th</sup> Session ESCAP/WMO Typhoon Committee*.
- [48] Moses, O. and Ramotonto, S., (2018). Assessing Forecasting Models on Prediction of the Tropical Cyclone Dineo and the Associated Rainfall Over Botswana. *Weather And Climate Extremes*, Vol. 21, 102-109. <https://doi.org/10.1016/j.wace.2018.07.004>.
- [49] MoNRE. (2017). Circular No. 41/2017/TT-BTNMT Promulgating Technical Regulations on Assessing the Quality of Meteorological Forecasting. *Ministry of Natural Resources and Environment*, Vietnam.
- [50] Heming, J. T., (2016). Tropical Cyclone Tracking and Verification Techniques for Met Office Numerical Weather Prediction Models. *Meteorological Applications*, Vol. 24(1), 1-8.
- [51] Chen, G., Li, T., Yang, M. and Zhang, X., (2023). Evaluation of Western North Pacific Typhoon Track Forecasts in Global and Regional Models During the 2021 Typhoon Season. *Atmosphere*, Vol. 14(3). <https://doi.org/10.3390/atmos14030499>.

- [52] Choquehuanca, B., Nieto, R. and García, E., (2025). Assessing the Skill of High-Impact Weather Forecasts in Southern South America: A Study on Cut-Off Lows. *Weather And Climate Dynamics*, Vol. 6, 317–327. <https://doi.org/10.5194/wcd-6-317-2025>.
- [53] Neumann, C. S. and Pelissier, J. M., (1981). An Analysis of Atlantic Tropical Cyclone Forecast Errors, 1970–1979. *Monthly Weather Review*, Vol. 109, 1248–1266.
- [54] Peng, X., Fei, J., Huang, X. and Cheng, X., (2017). Evaluation and Error Analysis of Official Forecasts of Tropical Cyclones during 2005–14 over the Western North Pacific. Part I: Storm Tracks. *Weather and Forecasting*. Vol. 32, 689–712.
- [55] Chaudhuri, S., Dutta, D., Goswami, S. and Middey, A., (2013). Intensity Forecast of Tropical Cyclones Over North Indian Ocean Using Multilayer Perceptron Model: Skill and Performance Verification. *Natural Hazards*, Vol. 65(1), 97–113. <https://doi.org/10.1007/s11069-012-0346-7>.
- [56] Knaff, J. A. and Zehr, R. M., (2007). Reexamination of Tropical Cyclone Wind–Pressure Relationships. *Weather Forecast*, Vol. 22, 71–88.
- [57] WMO. (2000). Guidelines on Performance Assessment of Public Weather Services.
- [58] Chan, P. W., Choy, C. W., He, J. Y. and Li, Q. S., (2022). An Observational Study of Super Typhoon Rai, a Very Late-Season Typhoon Necessitating the Issuance of a Tropical Cyclone Warning Signal for Hong Kong in December 2021. *Weather*, Vol. 77(12), 433–438. <https://doi.org/10.1002/wea.4202>.